RSC Advances

ROYAL SOCIETY OF CHEMISTRY

www.rsc.org/advances

Halogen-doping in $LiCoO_2$ cathode materials for Li-ion Batteries: insights from *ab initio* calculations

Guobao Li [1], Si Zhou[1*], Peng Wang [1], Jijun Zhao [1,2]

[1] *Key Laboratory of Materials Modification by Laser, Ion and Electron Beams (Dalian University of Technology), Ministry of Education, Dalian 116024, China*

[2] *Yangzhou Institute of Energy and Material, Chinese Academy of Sciences, Yangzhou 225127, China*

Abstract

Lithium cobalt oxide is one of the most commonly used cathode materials for Li ion batteries. However, the electrochemical cycling performance is limited by the structural instability of $LiCoO_2$ during the charging/discharging processes. Using density functional theory calculations, we investigate the effects of halogen doping on the structural stability, electronic state, electrode potential, and Li diffusion behavior of $LiCoO_2$ systems. Fluorine, chlorine, and bromine substitutions of oxygen species suppress the lattice changes upon Li deintercalation, enhance the structural stability, electronic conductivity and Li mobility, as well as retain electrode potential of the undoped system. Thus, halogen doping opens an effective route to improve the structural and electrochemical properties of $LiCoO_2$ cathodes for Li ion batteries with better rate capacity and longer lifetime.

* Corresponding author: Email: sizhou@dlut.edu.cn

1. Introduction

Rechargeable lithium-ion battery (LIB) is one of the most widely used energy conversion devices in portable electronics, and shows growing popularity in electric vehicles and aerospace applications. In LIBs, Li ions move between the electrodes during charging/discharging processes. The properties of electrode materials, such as structural stability, electrode potential, and mobility of Li ions, play the key roles in the electrochemical performance of LIBs. Lithium cobalt oxide ($LiCoO_2$) in the α-$NaFeO_2$ structure is a commercial cathode material in the current LIB industry [1, 2]. The layered structure of $LiCoO_2$ yields high rate capacity, satisfactory energy and power densities, and shows relatively good reversibility. A major problem limiting the cycling life of $LiCoO_2$ cathodes is the structural instability during charging/discharging. As shown in Fig. 1b, the lattice expansion rate along the *c* axis attains as much as 1.8% for ~50% delithiation degree, while the contraction rate is up to 10% for full delithiation [3-5]. This non-uniform lattice variation exceeds the elastic strain tolerance of ~0.1% for the cobalt oxides, leading to mechanical fracture and detrimental to the battery capacities on extended operation time [6-8].

Substitutional doping the Co sites with other metal ions has been exploited to enhance the structural stability of $LiCoO_2$ during the delithiation process [9-18]. Mg and La substitution of Co species has been demonstrated as an effective approach to retain the layered structure of $LiCoO_2$, suppress the phase transitions during Li interaction/deintercalation, and prominently improve the cycling performance of LIBs [19]. Dual-doped $LiCoO_2$ by Cu and Al species has been shown to process high degree of crystallinity with better phase purity. Compared to that of the pristine $LiCoO_2$, the doped materials exhibit lower capacity fade and higher columbic efficiency[20]. On the other hand, doping of Cr, V, Zr and Mo results in a deficient $LiCoO_2$ structure, and leads to irreversible capacity loss in the first cycle [18].

Alternatively, it is possible to substitutionally dope oxygen sites with nonmetal elements such as halogen, although less attention has been paid to this direction. It was found that fluorine substitution of oxygen species also affects the structural

properties of nickel and cobalt oxides [21-24]. F doping of $LiNiO_2$ has been shown to eliminate the abrupt changes of lattice distortion, and significantly improve the cycling life of LIBs[25]. $LiNi_xCo_yMn_{1-x-y}O_{2-z}F_z$ ($0 \le z \le 0.1$) compounds exhibit enhanced structural stability, in absence of phase transitions upon delithiation, and show excellent cycling performance and rate capacity than the fluorine-free compounds[26].

In this work, for the first time we explored the effects of halogen substitution of the oxygen sites in $LiCoO_2$ systems on the lattice variance during lithium deintercalation, electronic state, electrode voltage, and diffusion of Li ions using density functional theory (DFT) calculations. Our results show that the fluorine, chlorine and bromine doping correspond to n-type doping and increase the electron density of states at the Fermi level, which may partly enhance the electrical conduction, and facilitate the accommodation of Li ions in the compounds. The halogen substitution enhances the structural stability and helps improve the cycling life of battery by effectively suppressing the volume expansion rate by up to 0.7% and reducing the lattice contraction along the *c*-axis upon full delithiation by up to 3.2%. Moreover, halogen doping facilitates the migration of Li ions in the cathode material. Therefore, halogen substitution might be beneficial to the rate capacity and power density of LIBs.

2. Computational methods

DFT calculations were performed by using the Vienna Ab initio Simulation Package (VASP) [27, 28] with the projector-augmented wave (PAW) method[27, 29]. The valence electron states were expanded by a plane wave basis set with a kinetic energy cutoff of 500 eV. The generalized gradient approximation (GGA) parameterized by Perdew, Burke, and Ernzerhof (PBE) was adopted for the exchange-correlation functional [30]. To account for the strong correlation of the *d* electrons of cobalt, a Hubbard-like correction term (GGA+U) was included in the total energy functional. Since different U values for 3d of Co have been used for cobalt oxides [31, 32 33], here we have performed careful test and found that the choice of U=3 eV can reproduce the

experimental lattice parameter of $LiCoO_2$ (c_0=14.05 Å) [34].

The primitive unit cell of $LiCoO_2$ crystal consists of 12 atoms ($Li_3Co_3O_6$), as shown in Fig 1(a). The structure can be viewed as three cobalt oxide layers intercalated by Li atoms along the *c* axis. To model halogen-doped $LiCoO_2$ systems, a supercell of 5×5×1 unit cells containing a total of 300 atoms ($Li_{75}Co_{75}O_{150}$) with dimension of 14.15 Å × 14.15 Å × 14.05 Å was used. For the halogen doping, we randomly selected one oxygen atom on each layer, and replaced it with a halogen atom. As the halogen doping in experiment is very dilute, it is reasonable to assume the dopants distribute uniformly in the $LiCoO_2$ compound. For Li deintercalation, certain amount of Li atoms was randomly removed from the simulation supercell, modeling the homogeneous discharging process in reality. Due to the large supercell size, the Brillouin zone was sampled by the Γ point. The cell parameters and atomic coordinates were fully optimized until the force on each atom is less than 0.02 eV/Å. The climbing-image nudged elastic band (CI-NEB) method [35] was employed to search the saddle point and calculate the energy barrier for Li diffusion in the pristine and doped $LiCoO_2$ systems.

For pristine $LiCoO_2$ crystal, the computed lattice parameters of *a*=2.83 Å and *c*=14.05 Å coincide well with the experimental values (*a*=2.82Å and *c*=14.04~14.06 Å[3, 4, 34, 36]). To further test the validity of our computational scheme, we calculated the change of lattice parameter *c* of the pristine $LiCoO_2$ crystal during the delithiation process. As shown in Fig. 1b, the theoretical trend agrees excellently with the experimental one.

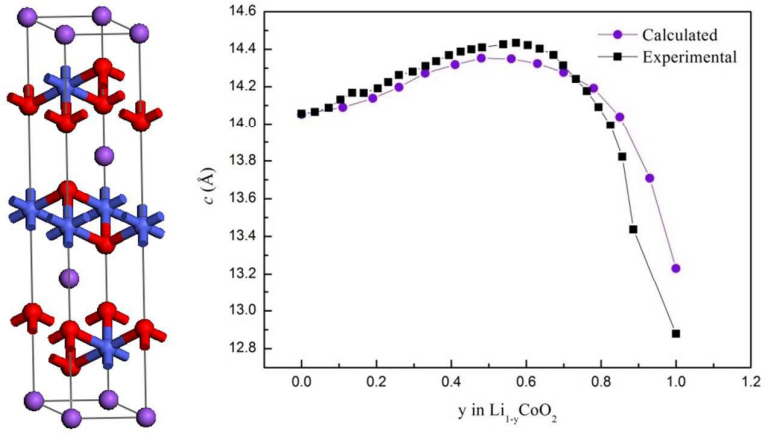

(a) (b)

Figure 1. (a) Ball-and-stick illustration of a $LiCoO_2$ unit cell. Li, Co and O species are represented in purple, blue and red, respectively. (b) The lattice parameter *c* vs. delithiation degree *y* of $Li_{1-y}CoO_2$ ($0 \leq y \leq 1$) from calculation (black) and the experimental data (blue).

3. Results and discussion

Structural properties

Table 1 lists the key structural parameters and substitution energy for doped $LiCoO_{1.96}X_{0.04}$ (X= F, Cl, Br) compounds, compared with the pristine $LiCoO_2$. Clearly, halogen doping of $LiCoO_2$ systems leads to lattice expansions in both the in-plane and out-of-plane directions. Upon doping, the lattice parameter *a* reflecting the Co-Co bond length, increases from 2.83 Å to 2.85 Å, and the lattice parameter *c* related to the interlayer distance, increases from 14.05 Å to 14.18 Å. The lattice extension in the *a* and *c* axis is attributed to the larger radii of partially reduced Co ions (0.55 Å for Co^{3+} and 0.65 Å for Co^{2+}) due to the charge compensation of halogen anion [22, 26]. Moreover, the larger ionic radii of Cl^- (1.81 Å) and Br^- (1.96 Å) species than that of O^{2-} (1.35 Å)[37] further increases the interlayer spacing along the *c* axis. In addition, the doped systems possess slightly higher *c*/*a* ratios, which means better layer properties [38, 39] and is beneficial for reversible charging/discharging processes [40, 41]. The larger cell volumes of doped structures yield higher capacity for lithium storage [42, 43], and is

helpful for improving the rate capacity and battery capacity of LIBs.

To characterize how difficult to substitute halogen species into the $LiCoO_2$ systems, we define the substitution energy E_{sub} as following

$$E_{sub} = \frac{[E(LiCoO_{1.96}X_{0.04} - E(LiCoO_2) + 0.02E(O_2) - 0.02E(X_2)]}{0.04}, \quad [1]$$

where $E(LiCoO_{1.96}X_{0.04})$ and $E(LiCoO_2)$ are the energies of halogen-doped and undoped $LiCoO_2$ systems, respectively; $E(O_2)$ and $E(X_2)$ are the energy of an O_2 molecule, and a F_2, Cl_2, or Br_2 molecule in the gas phase, respectively. Positive E_{sub} value means the substitution reaction is endothermic. We find that fluorine substitution of O in $LiCoO_2$ is relatively easy with E_{sub} of only 0.32 eV, while for Cl and Br doping, E_{sub} attains as much as 5 eV. Cl and Br doping show large E_{sub} values. Such process may be realized in experiment for low doping levels, for instance, by chemical or thermal treatment. Also, we might overestimated the E_{sub} values for Cl and Br doping, since the energies of stable Cl_2 and Br_2 molecules (rather than some reactive compounds) were used as reference. For comparisons, we calculated E_{sub} of some cation doping, i.e., Fe, Ni, and Cu substitution of Co sites, and obtained E_{sub}=1.5 eV, 2.35 eV, 1.73 eV, respectively, lying between F–doping and Cl–, Br–doping. Although Cl and Br doping are relatively more difficult, they can still be realized under elaborately designed experimental conditions.

Table 1. The lattice parameters *a* and *c*, *c*/*a* ratio, unit cell volume *V*, and substitution energy (E_{sub}) for $LiCoO_2$ and $LiCoO_{1.96}X_{0.04}$ (X= F, Cl and Br) solids.

Models	*a* (Å)	*c* (Å)	*c*/*a*	V (Å^3)	E_{sub} (eV)
$LiCoO_2$	2.83	14.05	4.96	97.45	—
$LiCoO_{1.96}F_{0.04}$	2.84	14.11	4.97	98.56	0.32
$LiCoO_{1.96}Cl_{0.04}$	2.85	14.14	4.96	99.18	3.88
$LiCoO_{1.96}Br_{0.04}$	2.85	14.18	4.98	99.88	5.34

To explore the effect of halogen doping on the volume change of $LiCoO_2$ during the delithiation process, we calculated the lattice parameters of the systems with various Li contents. The lattice parameter *a* shows little change by varying the Li

concentration. On the contrary, the lattice parameter c of $Li_{1-y}CoO_{1.96}X_{0.04}$ ($0 \leq y \leq 1$) first increases with the delithiation degree y, achieving the maximum at $y \sim 0.5$, and then decreases with further delithiation (Fig. 2). The expansion along the c axis for $y < 0.5$ is attributed to the increased electrostatic repulsions between CoO_2 layers due to the removal of Li ions [44]. For Li contents below 0.5, the screening effect cannot compete with interlayer binding, and hence the system contracts along the c axis.

The volume expansion/contraction during the delithiation process can be characterized by the c/c_0 ratio, where c_0 is the lattice parameter for full lithium intercalation (y=0). As shown in Fig. 2a, fluorine doping effectively inhibits the volume change for a wide range of delithiation degree ($0.3<y<0.7$). In particular, the maximum volume expansion is suppressed to 1.4% for $Li_{1-y}CoO_{1.96}F_{0.04}$, in comparison with 2.1% for $Li_{1-y}CoO_2$, mainly due to the smaller ionic radii of F^- than that of O^{2-}. At full delithiation degree, the volume contracts by 4.8% for $CoO_{1.96}F_{0.04}$, compared with 5.6% for CoO_2, due to the larger F-Co bond length (2.00 Å) than O-Co (1.87 Å). For chlorine and bromine doping, the volume expansion is almost the same as that of the undoped system (maximum expansion at 2.5% for $Li_{1-y}CoO_{1.96}Cl_{0.04}$ and 2.4% for $Li_{1-y}CoO_{1.96}Br_{0.04}$). More importantly, the contraction at full delithiation degree drops to 2.7% for Cl doping and 2.4% for Br doping, respectively. Overall speaking, suppression of volume expansion and contraction of $Li_{1-y}CoO_{1.96}X_{0.04}$ compounds helps retain the structural stability and capacity of the systems, allows deep charging for y>0.5, and hence improves the electrochemical cycling performance of LIBs.

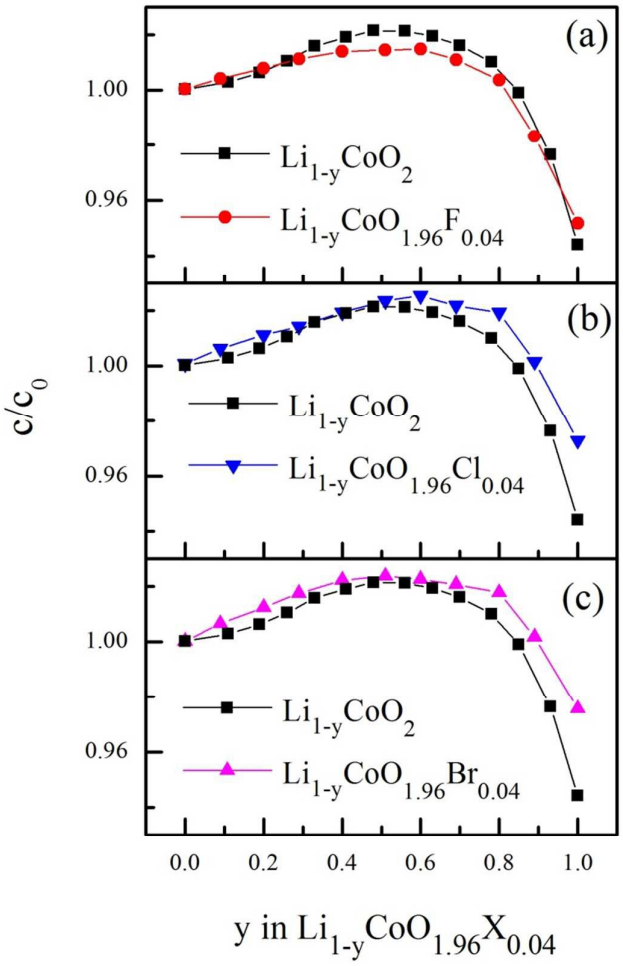

Figure 2. The c/c_0 ratio vs. the delithiation degree y for $Li_{1-y}CoO_2$ (black), and $Li_{1-y}CoO_{1.96}X_{0.04}$ (colored), where X=F (a), Cl (b), Br (c).

To characterize the structural stability of $Li_{1-y}CoO_{1.96}X_{0.04}$ systems from the thermodynamic point of view, we defined the formation energy E_{form} as[45]:

$$E_{\text{form}} = E\left(\text{Li}_{1-y}\text{CoO}_{1.96}\text{X}_{0.04}\right) - (1-y)E(\text{LiCoO}_{1.96}\text{X}_{0.04}) - yE(\text{CoO}_{1.96}\text{X}_{0.04}) \quad [2]$$

where $E(Li_{1-y}CoO_{1.96}X_{0.04})$, $E(LiCoO_{1.96}X_{0.04})$, and $E(CoO_{1.96}X_{0.04})$ are the energies of the system with delithiation degree y, full lithium interaction, and full delithiation, respectively. Positive E_{form} means the $Li_{1-y}CoO_{1.96}X_{0.04}$ compound during Li deintercalation is unstable; the system favors phase separation into the fully Li intercalated compound $LiCoO_{1.96}X_{0.04}$ and doped cobalt oxide $CoO_{1.96}X_{0.04}$. The structural instability and phase transition during charging/discharging is a general

problem for $LiCoO_2$ compounds used for the cathodes of Li-ion batteries. As shown in Fig. 3, for all degrees of delithiation, both the doped and undoped systems have negative formation energies, and the formation energy achieves the minimum at y=0.5, indicating the preference of the system in the form of $Li_{1-y}CoO_{1.96}X_{0.04}$ compound, rather than phase separation into $LiCoO_{1.96}X_{0.04}$ and $CoO_{1.96}X_{0.04}$ forms. Most impressively, the doped systems have lower formation energies than that of undoped ones by about 100 meV for $0.2 \leq y \leq 0.6$, showing the enhanced structural stability after halogen doping.

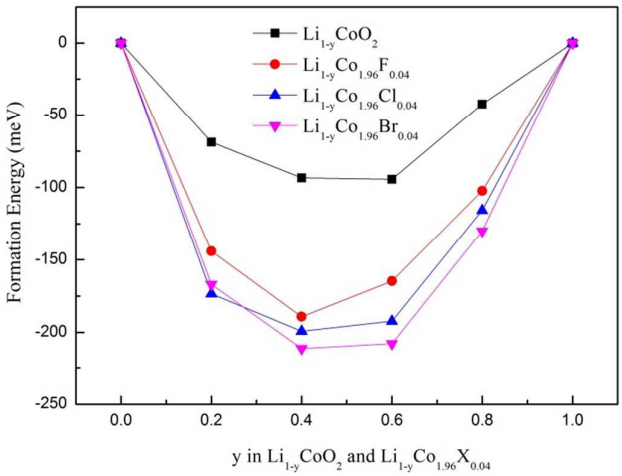

Figure 3. The formation energies vs. the delithiation degree y for $Li_{1-y}CoO_{1.96}X_{0.04}$ and $Li_{1-y}CoO_2$ systems, where X=F, Cl, Br.

Electronic structure and electrode potential

In contrast to the significant impacts on the structural properties, halogen doping does not affect much the electronic state of $LiCoO_2$ systems. As seen from the total density of states (TDOS) in Fig. 4, both doped and undoped $LiCoO_2$ compounds exhibit a semiconductor character with a band gap of about 1.1 eV. The calculated band gap of $LiCoO_2$ agrees well with previous theoretical results of 1.2 eV [46], but is smaller than the experimental value of 2.7 eV [47], as a well-known deficiency of conventional GGA functional.

For pristine $LiCoO_2$, three main bands of can be identified[46]. The valence band in

the range from −7.3 to −2.6 eV is originated from the O-2p orbital hybridized with the Co-3d orbital, corresponding to strong Co-O covalent bonding. The energy states ranging from −2.3 to −0.7eV and 0.7 to 1.5 eV are attributed to the t_{2g} states and the e_g states of the Co-3d orbital, respectively. These bands for the doped compounds are similar to that of pure $LiCoO_2$. The Fermi energy has shifted to the bottom of conduction band upon halogen doping, and some additional states emerge around the Fermi energy, indicating *n*-type doping. Definitely, these states around Fermi energy are beneficial for accommodating electrons during lithium extraction/insertion to decrease the polarization potential[48].

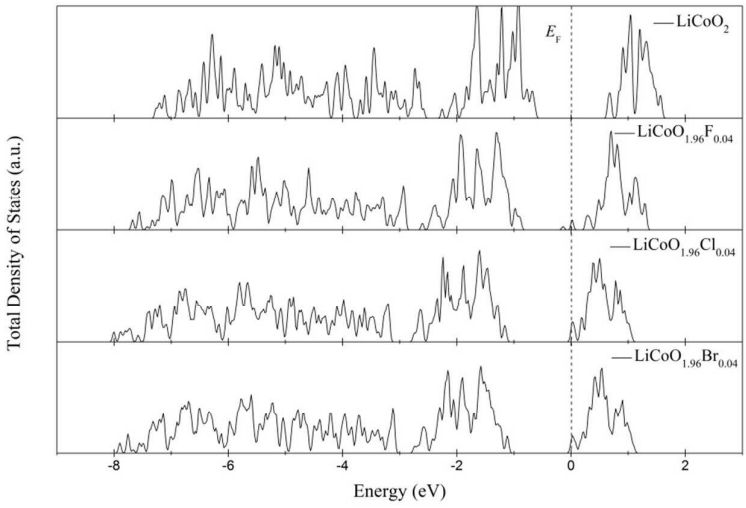

Figure 4. The total density of states (TDOS) of undoped and halogen-doped $LiCoO_2$ compounds. The zero energy level indicated by the dotted line is referred to the Fermi energy (E_F).

In the computional simulation of electrode materials, the average electrode potential *U* as the delithiation degree varies from y_1 to y_2 ($y_1<y_2$) can be estimated by the following equation[49]:

$$U = \frac{E\left(\mathrm{Li}_{1-y_2}\mathrm{CoO}_{1.96}\mathrm{X}_{0.04}\right) + (y_2 - y_1)E_{\mathrm{Li}} - E\left(\mathrm{Li}_{1-y_1}\mathrm{CoO}_{1.96}\mathrm{X}_{0.04}\right)}{(y_2 - y_1)e} \qquad [3]$$

where $E(\mathrm{Li}_{1-y1}\mathrm{CoO}_{1.96}\mathrm{X}_{0.04})$ and $E(\mathrm{Li}_{1-y2}\mathrm{CoO}_{1.96}\mathrm{X}_{0.04})$ are the energies of the system with delithiation degrees of y_1 and y_2, respectively; E_{Li} is the energy per Li atom in the

BCC solid phase; e is the electron charge. The electrode potential curves for $Li_{1-y}CoO_{1.96}X_{0.04}$ with the delithiation degree y are displayed in Fig. 5, and the average electrode potential $\bar{U}$ ($0 \leq y \leq 1$) are shown in Table 2. The computed value of $\bar{U}$ = 4.1 V for the pristine $LiCoO_2$ is in good agreement with the experimental values of 3.9~4.21 V [4, 36, 50]. From Fig. 5, we can see the electrode potential for the doped materials are relative lower by about 0.6 V, compared to that of the pristine system in the initial delithiation degree y ($0 \leq y \leq 0.2$). But in the whole y range, the differences of $\bar{U}$ between doped and pristine systems are within 0.2 V (3.9~4.0 V for halogen doping materials, shown in Table 2). Therefore, halogen doping basically does not deteriorate the electrode potential of $LiCoO_2$ cathodes.

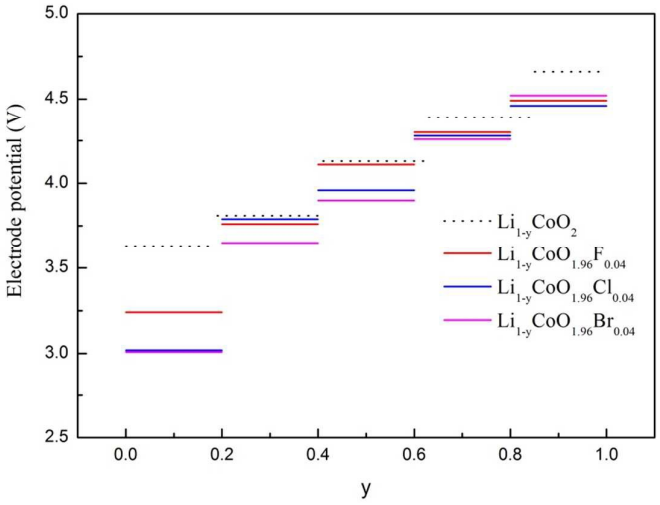

Figure 5. The electrode potential curves (vs. Li/Li^+) for $Li_{1-y}CoO_{1.96}X_{0.04}$ vs. the delithiation degree y.

Table 2. The average electrode potential $\bar{U}$ with the delithiation degree y ranging from 0 to 1 for the halogen-doped and undoped $LiCoO_2$ systems.

	$Li_{1-y}CoO_2$	$Li_{1-y}CoO_{1.96}F_{0.04}$	$Li_{1-y}CoO_{1.96}Cl_{0.04}$	$Li_{1-y}CoO_{1.96}Br_{0.04}$
$\bar{U}$ (V)	4.1	4.0	3.9	3.9

Lithium diffusion

Fast migration of Li ions in the host materials is of great importance to achieve high

battery power. Previous theoretical studies have shown that the tetrahedral site hop (TSH) mechanism involving a lithium divacancy is dominant for most Li concentrations [51, 52]. In this scenario, a Li ion moves from one octahedral site to an adjacent Li vacancy site by passing through the center of the tetrahedron formed by the O species of two neighboring CoO_2 layers, while keeping away from the dopant sites, as illustrated in Fig. 6. According to the present method, the maximum energy along the minimum energy path between two neighboring Li sites is defined as activation energy.

The calculated activation energies of Li ion in pristine and doped $LiCoO_2$ solids are summarized in Table 3. The activation energy for Li migration in pristine $LiCoO_2$ is 0.21 eV, in good agreement with the previous computational results of 0.22 eV obtained from LDA and the Monte Carlo simulations [51, 52]. For some other lithium transition metal oxides $LiMO_2$ (M=Ni, Cu, Co, Mn), the calculated activation energies range from 0.21 eV to 0.49 eV [53, 54], which are slight higher than that of pristine $LiCoO_2$. For the cation doping of $LiCoO_2$, such as $LiMn_xNi_yCo_{1-x-y}O_2$ compounds, the activation energies range from 0.34 eV to 1.23 eV from the previous DFT calculations [40], suggesting that the migration of Li species is unflavored because the combined effects of O–TM distance along *c* direction as well as the electrostatic interaction between Li^+ ion in the activated state and the transition metal cation directly below it. In contrast, for the anion doped systems in this study, the activation energies are significantly reduced, from 0.20 eV for F doping, to 0.12 eV for Cl doping and down to 0.09 eV for Br doping, shown in Table 3. The small activation energy for Li diffusion upon halogen doping may be mainly attributed to the lattice expansion along the *c*–axis, which facilitates the transport of Li species in–between the cobalt oxide layer [55]. Therefore, halogen doping facilitates the migration of Li species in the $LiCoO_2$ compounds, and helps improve the battery power of LIBs.

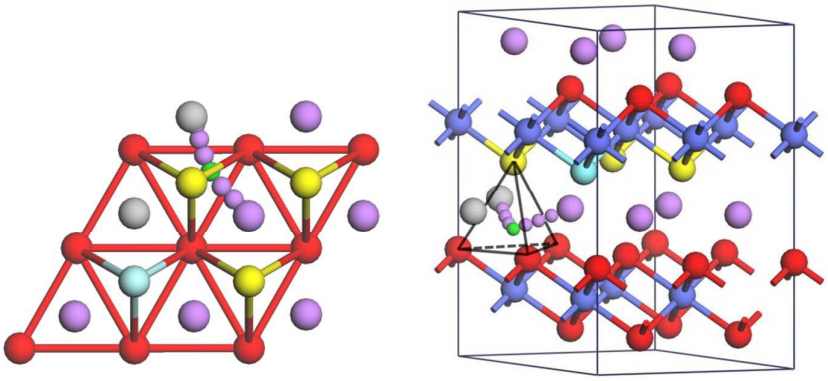

(a) (b)

Figure 6. The diffusion pathway for a Li ion to migrate from one equilibrium site to a neighboring Li vacancy site: top view (a), and side view (b). The two Li vacancies are represented by the gray balls. The intermediate states and the transition state are indicated by the small purple and green balls, respectively. Li, Co, O, and halogen species are represented by purple, blue, red and light blue balls, respectively. The yellow balls show the O species on the upper CoO_2 layer forming tetrahedrons (indicated by the black lines in the side view) with the O species on the bottom CoO_2 layer.

Table 3. The calculated activation energies for lithium diffusion in the halogen-doped and undoped $LiCoO_2$ systems.

	$LiCoO_2$	$LiCoO_{1.96}F_{0.04}$	$LiCoO_{1.96}Cl_{0.04}$	$LiCoO_{1.96}Br_{0.04}$
E_a (eV)	0.21	0.20	0.12	0.09

4. Conclusions

The effects of halogen doping on the structural stability, electronic state, electrode potential, and lithium diffusion of $LiCoO_2$ cathode materials have been investigated by DFT calculations. Fluorine, chlorine, and bromine substitution of oxygen species with a doping concentration of O:X = 1.96:0.04 (X=F, Cl and Br) are considered. Our studies show that halogen doping has positive effect on the electronic conductivity, and does not deteriorate the electrode potential of $LiCoO_2$ systems. The halogen

species induces enlarged Li slabs, helps improve the capacity for lithium storage, and facilitates the migration of lithium ions inside the $LiCoO_2$ compounds. Most importantly, halogen doping inhibits the lattice change along the *c* axis during the delithiation process, i.e., the maximum lattice extension rate c/c_0 is reduced by up to 0.7%, and the lattice contraction rate at full delithiation is lowered by up to 3.2% compared to the undoped system. The suppression of volume variance helps retaining the structural stability and capacity of the $LiCoO_2$ cathodes during the charging/discharging processes. All these results indicate that halogen doping of $LiCoO_2$ cathodes is an effective approach to enhance the rate capacity and battery power, as well as to improve the electrochemical cycling performance of LIBs.

Acknowledgements

This work was supported by the China Postdoctoral Science Foundation (2015M570243), the National Natural Science Foundation of China (11504041), the Fundamental Research Funds for the Central Universities of China (DUT15RC(3)014), Liaoning BaiQianWan Talents Program (2014921021), and the Natural Science Foundation of Jiangsu Province (BK2012255, BY2013064, BK20130458, BK20130431).

Notes and references

1. K. Mizushima, P. Jones, P. Wiseman and J. B. Goodenough, *Materials Research Bulletin*, 1980, **15**, 783-789.

2. T. Nagaura and K. Tozawa, *Prog. Batteries Solar Cells*, 1990, **9**, 209.

3. J. N. Reimers and J. Dahn, *Journal of the Electrochemical Society*, 1992, **139**, 2091-2097.

4. G. Amatucci, J. Tarascon and L. Klein, *Journal of The Electrochemical Society*, 1996, **143**, 1114-1123.

5. T. Ohzuku and A. Ueda, *Journal of The Electrochemical Society*, 1994, **141**, 2972-2977.

6. H. Wang, Y. I. Jang, B. Huang, D. R. Sadoway and Y. M. Chiang, *Journal of the Electrochemical Society*, 1999, **146**, 473-480.

7. K. Dokko, M. Nishizawa, S. Horikoshi, T. Itoh, M. Mohamedi and I. Uchida, *Electrochemical and Solid-State Letters*, 2000, **3**, 125-127.

8. M. Thackeray, *Journal of The Electrochemical Society*, 1995, **142**, 2558-2563.

9. J. W. Fergus, *Journal of Power Sources*, 2010, **195**, 939-954.

10. M. Reddy, T. W. Jie, C. J. Jafta, K. I. Ozoemena, M. K. Mathe, A. S. Nair, S. S. Peng, M. S. Idris, G. Balakrishna and F. I. Ezema, *Electrochimica Acta*, 2014, **128**, 192-197.

11. S. Gopukumar, Y. Jeong and K. B. Kim, *Solid State Ionics*, 2003, **159**, 223-232.

12. C. Jones, E. Rossen and J. Dahn, *Solid State Ionics*, 1994, **68**, 65-69.

13. C. Julien, M. Camacho-Lopez, T. Mohan, S. Chitra, P. Kalyani and S. Gopukumar, *Solid State Ionics*, 2000, **135**, 241-248.

14. I. Saadoune and C. Delmas, *Journal of Solid State Chemistry*, 1998, **136**, 8-15.

15. H. Kobayashi, H. Shigemura, M. Tabuchi, H. Sakaebe, K. Ado, H. Kageyama, A. Hirano, R. Kanno, M. Wakita and S. Morimoto, *Journal of the Electrochemical Society*, 2000, **147**, 960-969.

16. M. Zou, M. Yoshio, S. Gopukumar and J.-i. Yamaki, *Chemistry of materials*, 2003, **15**, 4699-4702.

17. M. Zou, M. Yoshio, S. Gopukumar and J.-i. Yamaki, *Chemistry of materials*, 2005, **17**, 1284-1286.

18. S. Needham, G. Wang, H. Liu, V. Drozd and R. Liu, *Journal of Power Sources*, 2007, **174**, 828-831.

19. X. Zhu, K. Shang, X. Jiang, X. Ai, H. Yang and Y. Cao, *Ceramics International*, 2014, **40**, 11245-11249.

20. R. Thirunakaran, T. Kim and W.-s. Yoon, *Journal of Applied Electrochemistry*, 2014, **44**, 709-718.

21. G. G. Amatucci and N. Pereira, *Journal of Fluorine Chemistry*, 2007, **128**, 243-262.

22. G.-H. Kim, J.-H. Kim, S.-T. Myung, C. Yoon and Y.-K. Sun, *Journal of the Electrochemical Society*, 2005, **152**, A1707-A1713.

23. S.-W. Oh, S.-H. Park, J.-H. Kim, Y. C. Bae and Y.-K. Sun, *Journal of power sources*, 2006, **157**, 464-470.

24. A. Naghash and J. Y. Lee, *Electrochimica acta*, 2001, **46**, 2293-2304.

25. K. Kubo, M. Fujiwara, S. Yamada, S. Arai and M. Kanda, *Journal of power sources*, 1997, **68**, 553-557.

26. S. H. Lee, J.-S. Moon, M.-S. Lee, T.-H. Yu, H. Kim and B. M. Park, *Journal of Power Sources*, 2015, **281**, 77-84.

27. G. Kresse and J. Furthmüller, *Computational Materials Science*, 1996, **6**, 15-50.

28. G. Kresse and J. Hafner, *Physical Review B*, 1993, **48**, 13115.

29. P. E. Blöchl, *Physical Review B*, 1994, **50**, 17953.

30. J. P. Perdew, K. Burke and M. Ernzerhof, *Physical review letters*, 1996, **77**, 3865.

31. S. Laubach, S. Laubach, P. C. Schmidt, D. Ensling, S. Schmid, W. Jaegermann, A. Thißen, K. Nikolowski and H. Ehrenberg, *Physical Chemistry Chemical Physics*, 2009, **11**, 3278-3289.

32. K.-W. Lee and W. Pickett, *Physical Review B*, 2005, **72**, 115110.

33. F. Zhou, M. Cococcioni, C. A. Marianetti, D. Morgan and G. Ceder, *Physical Review B*, 2004, **70**, 235121.

34. W. Johnston, R. Heikes and D. Sestrich, *Journal of Physics and Chemistry of Solids*, 1958, **7**, 1-13.

35. G. Henkelman, B. P. Uberuaga and H. Jónsson, *The Journal of chemical physics*, 2000, **113**, 9901-9904.

36. T. Ohzuku, A. Ueda, M. Nagayama, Y. Iwakoshi and H. Komori, *Electrochimica Acta*, 1993, **38**, 1159-1167.

37. R. t. Shannon, *Acta Crystallographica Section A: Crystal Physics, Diffraction, Theoretical and General Crystallography*, 1976, **32**, 751-767.

38. J.-H. Kim, C. Park and Y.-K. Sun, *Solid State Ionics*, 2003, **164**, 43-49.

39. J. K. Ngala, N. A. Chernova, M. Ma, M. Mamak, P. Y. Zavalij and M. S. Whittingham, *Journal of materials chemistry*, 2004, **14**, 214-220.

40. G. Luo, J. Zhao, X. Ke, P. Zhang, H. Sun and B. Wang, *Journal of The Electrochemical Society*, 2012, **159**, A1203-A1208.

41. H.-G. Jung, N. V. Gopal, J. Prakash, D.-W. Kim and Y.-K. Sun, *Electrochimica Acta*, 2012, **68**, 153-157.

42. L. Wang, J. Li, X. He, W. Pu, C. Wan and C. Jiang, *Journal of Solid State Electrochemistry*, 2009, **13**, 1157-1164.

43. P. Ghosh, S. Mahanty and R. N. Basu, *Materials Chemistry and Physics*, 2008, **110**, 406-410.

44. A. Van der Ven, M. Aydinol, G. Ceder, G. Kresse and J. Hafner, *Physical Review B*, 1998, **58**, 2975.

45. A. Dianat, N. Seriani, M. Bobeth and G. Cuniberti, *Journal of Materials Chemistry A*, 2013, **1**, 9273-9280.

46. Y. Takahashi, N. Kijima, K. Tokiwa, T. Watanabe and J. Akimoto, *Journal of Physics: Condensed Matter*, 2007, **19**, 436202.

47. J. Van Elp, J. Wieland, H. Eskes, P. Kuiper, G. Sawatzky, F. De Groot and T. Turner, *Physical Review B*, 1991, **44**, 6090.

48. G. Luo, J. Zhao and B. Wang, *Journal of Renewable and Sustainable Energy*, 2012, **4**, 063128.

49. M. Aydinol, A. Kohan, G. Ceder, K. Cho and J. Joannopoulos, *Physical Review B*, 1997, **56**, 1354.

50. T. Ohzuku and A. Ueda, *Journal of The Electrochemical Society*, 1997, **144**, 2780-2785.

51. A. Van der Ven and G. Ceder, *Electrochemical and Solid-State Letters*, 2000, **3**, 301-304.

52. A. Van der Ven, G. Ceder, M. Asta and P. Tepesch, *Physical Review B*, 2001, **64**, 184307.

53. K. Kang, Y. S. Meng, J. Bréger, C. P. Grey and G. Ceder, *Science*, 2006, **311**, 977-980.

54. Y. S. Meng and M. E. Arroyo-de Dompablo, *Energy & Environmental Science*, 2009, **2**, 589-609.

55. K. Kang and G. Ceder, *Physical Review B*, 2006, **74**, 094105.

Graphical Abstract